Vortex Pinning Properties of Dense Ti-Doped MgB_2 Bulks Sintered at Different Temperatures

Tomoyuki Naito, Takafumi Yoshida, Hidehiko Mochizuki, Hiroyuki Fujishiro, Ritwik Basu, and Jerzy A. Szpunar

***Abstract*—We have studied the trapped field by field-cooled magnetization and microstructure of the Ti-doped MgB_2 bulks fabricated at 700 °C by an *in situ* hot isostatic pressing method, which were compared with those at 900 °C. The maximum trapped field B_T of 3.0 T at 19 K was realized at the Ti-doping level of 10%–20%. In spite of the lower filling factor of 700 °C Ti-doped bulks, i.e., $f \sim 80\%$, the obtained $B_T = 3.0$ T was 1.3 times larger than that of the nondoped bulk ($f \sim 90\%$) and was comparable with those for the 900 °C Ti-doped bulks ($f \sim 90\%$) with the same Ti contents. The quantitative analysis of the chemical composition revealed that fine particles of higher borides, i.e., MgB_y ($y > 2$), existed in the MgB_2 matrix. The low sintering temperature of 700 °C and the Ti doping strongly suppressed the grain growth of the MgB_2 matrix. The increase in both the grain boundaries of MgB_2 and the nonsuperconducting fine particles enhanced the trapped field of the present 700 °C Ti-doped MgB_2 bulks.**

***Index Terms*—Critical current density, electron backscattered diffraction (EBSD), field-cooled magnetization (FCM), MgB_2, superconducting bulk magnet, Ti doping, trapped magnetic field.**

I. Introduction

SUPERCONDUCTING bulk magnets with a Tesla-order trapped magnetic field, B_T, are very promising for developments of a novel superconducting apparatus [1], in which the B_T is used in an open space as a conventional permanent magnet. In addition to single grain RE-Ba-Cu-O (RE is rare earth element) bulk magnets, MgB_2 bulk magnets have been extensively studied, especially for recent years [2]–[8]. This is because the specific features of MgB_2 including weak-link-free grain boundaries [9], [10], RE free, light weight and high yield stress [11] possibly overcome the shortcomings of RE-Ba-Cu-O bulks.

Major problems of MgB_2 are a low filling factor, f, of about 50–75% of the theoretical density and a strongly suppressed critical current density, J_c, in magnetic fields. Highly dense MgB_2 can be achieved by a sintering under high pressure [12], [13]. We have reported that the trapped field by field-cooled magnetization (FCM) was enhanced from 1.5 T for the porous MgB_2 bulk ($f \sim 50\%$) sintered at $T_{\rm sin} = 900$ °C under an ambient pressure [4] to 2.5 T for the dense bulk ($f \sim 90\%$) fabricated at the same $T_{\rm sin}$ by a hot isostatic pressing (HIP) method [6]. The increase in both the cross-section of the supercurrent path and the number density of grain boundaries acting as the pinning centers enhanced the B_T. Fuchs *et al.* realized B_T of 5.4 T at 12 K for the uniaxially hot pressed MgB_2 bulk using the nanometric ball-milled MgB_2 powder [14], demonstrating that the simultaneous grain refining and densification are quite effective to enhance the B_T. The introduction of pinning centers by chemical doping is an another route to improve the vortex pinning properties. $Mg_{1-x}Ti_xB_2$ sample with $x = 0.1$ synthesized at the ambient pressure demonstrated the enhanced J_c of 10^6 A cm^{-2} at 20 K in the self-field, which was about three orders of magnitude larger than that of the $x = 0$ sample [15]. This originated from the fact that the TiB_2 phase with lamellar structure at the boundaries of MgB_2 grains suppressed concurrently the grain growth of MgB_2 and the creation of MgB_4 impurity phase at the grain boundaries [16]. We reported the trapped field properties of the highly dense Ti-doped MgB_2 bulks sintered in the HIP furnace at $T_{\rm sin} = 900$ °C [8]. B_T of 3.6 T was obtained at 13 K on the surface for the Ti5–20%-doped bulks, which was 1.3 times larger than that of the pristine bulk. The higher B_T of 4.6 T was realized at 14 K in the pair of Ti5% and Ti10%-doped bulks due to the elimination of the demagnetization effect. The element maps obtained by an electron probe micro-analyzer suggested that the nanometric particles of unreacted B, Mg-B and TiB_2 were expected to act as the strong pinning centers in high magnetic fields. As found in several reports, the oxygen also plays an important role on the J_c-increase [17], [18]. The nanometric MgO and B- and O-enriched inclusions acted as the pinning centers [17], [18], and Ti-doping assisted the formation of such nanostructures and offered the further increase in J_c [18]. The volume fraction and the size of the nanometric particles might depend on the fabricating temperature. In this paper, we have fabricated Ti-doped MgB_2 bulks at $T_{\rm sin} = 700$ °C by HIP method and investigated the trapped field properties and microstructure which were compared to those of the Ti-doped bulks fabricated at $T_{\rm sin} = 900$ °C.

II. Experimental Procedure

A. MgB_2 Bulk Preparation

Ti-doped MgB_2 bulks were fabricated by an *in situ* HIP method, which was detailed elsewhere [8]. The nominal

Manuscript received September 8, 2015; accepted February 9, 2016. Date of publication February 23, 2016; date of current version April 25, 2016. This work was supported in part by Hitachi Metals·Materials Science Foundation and in part by JSPS KAKENHI Grants 23560002, 15K04718, and 15K04646.

T. Naito, T. Yoshida, H. Mochizuki, and H. Fujishiro are with the Faculty of Engineering, Iwate University, Morioka 020-8551, Japan (e-mail: tnaito@iwate-u.ac.jp).

R. Basu is with the Department of Mechanical Engineering, The Northcap University, Gurgaon-122 017, India.

J. A. Szpunar is with the Department of Mechanical Engineering, University of Saskatchewan, Saskatoon, SK S7N 5A9, Canada.

Color versions of one or more of the figures in this paper are available online at http://ieeexplore.ieee.org.

Digital Object Identifier 10.1109/TASC.2016.2531426

TABLE I
SPECIFICATIONS OF THE MEASURED MgB_2 BULKS

Bulk name	Sintering temperature, T_{sin}=700 °C							T_{sin}=900 °C	
	pristine	Ti1%	Ti5%	Ti10%	Ti20%	Ti30%	Ti50%	pristine	Ti10%
Critical temperature, T_c (K)	38.2	38.3	38.3	38.3	38.3	38.3	37.7	38.1	38.3
Filling factor, f (%)	87	88	81	79	75	73	68	94	92
Volume fraction of MgB_2, V_f (%)	87	87	77	72	62	53	36	94	84

composition of the precursors was $Mg:Ti:B = (1-x):x:2$ ($x = 0, 0.01, 0.05, 0.1, 0.2, 0.3, 0.5$) in molar ratio. The precursor pellet sealed in the evacuated stainless steel container was sintered at $T_{sin} = 700$ °C for 3 h under an argon-gas pressure of 98 MPa and cooled down to the room temperature by furnace cooling. The MgB_2 disk-bulks with 38 mm in diameter and 7 mm in thickness were machined. The critical temperatures, T_c's, were about 38 K for all the bulks, which were determined at the mid-point of the transition in the magnetization curve, $M(T)$. The filling factor of the bulk, f, which was the ratio of the measured mass density to the theoretical one of the MgB_2-Ti composite, was 87% for the pristine bulk, decreased monotonically with increasing Ti-content, and finally degraded to 68% for the Ti50% bulk, which is contrast to the larger f over 90% for the bulks sintered at 900 °C. We also estimated the volume fraction, V_f, of the MgB_2 phase in the bulks. The specification of the measured MgB_2 bulks are shown in Table I.

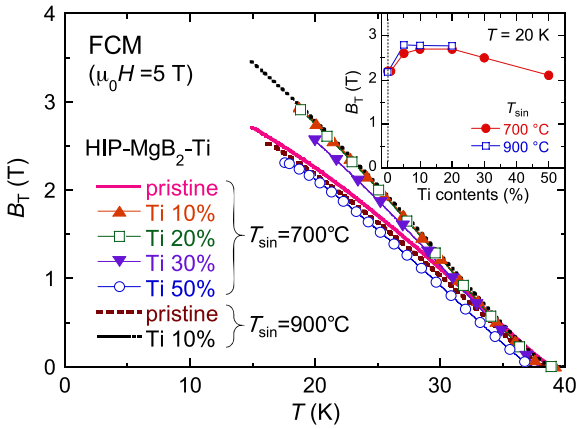

Fig. 1. Temperature dependence of the trapped field, $B_T(T)$, of the pristine and four Ti-doped MgB_2 bulks sintered at $T_{sin} = 700$ °C. The $B_T(T)$ curves of the MgB_2 bulks ($x = 0$ and 0.1) fabricated at $T_{sin} = 900$ °C are also shown, which are referred to in Ref. [8]. Inset shows the trapped field at 20 K as a function of Ti contents for MgB_2 bulks with $T_{sin} = 700$ °C and 900 °C.

B. Measurements

The experimental setup of the FCM is as follows. The MgB_2 bulk was set on the cold-stage of the G-M type cryocooler by inserting a thin indium sheet. A Pt-Co thermometer and 50 W heater were employed to control the temperature of the cold-stage and a Cernox thermometer to monitor the temperature of the bulk surface. The MgB_2 bulk was magnetized by FCM around 15 K under an external magnetic-field of $\mu_0 H = 5$ T parallel to the thickness direction. After the $\mu_0 H$ was decreased to 0 T at a rate of 0.022 T min^{-1}, the trapped field, B_T, was measured at the center of the bulk surface using a cryogenic Hall sensor (HP-VVP, AREPOC s.r.o.). During FCM, the temperature rise on the bulk surface was as small as 0.1 K for all the bulks. The temperature and magnetic-field dependences of magnetization, $M(T)$, and $M(\mu_0 H)$, were measured by a SQUID magnetometer (MPMS-XL, Quantum Design, Inc.) using a small piece cut from the bulk. The critical current density, J_c, was estimated from the $M(\mu_0 H)$ loop using the extended Bean model [19], [20]. The microstructure and chemical composition of bulks were analyzed by an electron probe micro-analyzer with a field emission gun (FE-EPMA) and a scanning electron microscopy (SEM) coupled with electron backscatter diffraction (EBSD).

III. RESULTS AND DISCUSSION

Fig. 1 shows the temperature dependence of the trapped field, $B_T(T)$, of the $Mg_{1-x}Ti_xB_2$ bulks ($x = 0, 0.1, 0.2, 0.3, 0.5$) sintered at $T_{sin} = 700$ °C. The $B_T(T)$ curves of the $Mg_{1-x}Ti_xB_2$ bulks with $T_{sin} = 900$ °C for $x = 0$ and 0.1 are also depicted for comparison, which are referred to in Ref. [8]. Hereafter, the bulks fabricated at $T_{sin} = 700$ °C and 900 °C are denoted using the prefixes "700d-" and "900d-", respectively. The B_T of 2.7 T was obtained for the 700d-pristine bulk at the lowest temperature of 14.8 K, was decreased monotonically with elevating temperature, and finally reached zero at $T_c = 38$ K. The B_T of 2.7 T for the pristine bulk was enhanced to 3.5 T for the Ti10–20%-doping. However, the B_T decreases for the Ti30% and B_T for Ti50%-doping is lower than that of 700d-pristine bulk. Inset of Fig. 1 shows the Ti-content dependence of B_T at 20 K for both 700d- and 900d-bulks. The B_T seems to be insensitive to the sintering temperature T_{sin}. The B_T is maximized at the wide optimal Ti-contents of 10–20%, which is inconsitent with the optimal doping level of 10% in previous reports [15], [21].

Fig. 2(a) shows the magnetic field dependence of the critical current density, $J_c(\mu_0 H)$, at 20 K for the 700d-MgB_2 bulks. The $J_c(\mu_0 H)$'s of the 900d-bulks with $x = 0$ and 0.1 are also plotted [8]. The moderate decay of $J_c(\mu_0 H)$ was observed above 3 T for the 700d-pristine bulk in contrast to that of the 900d-pristine bulk. Especially, the irreversibility field, $\mu_0 H_{irr}$, of the 700d-pristine bulk evidently exceeds 5 T, which is defined as the magnetic field for $J_c = 10$ A cm^{-2}. The $J_c(\mu_0 H)$ curves of the Ti-doped bulks seem not to depend strongly on neither the sintering temperature nor Ti-contents, except for the Ti50%-doping. The J_c versus Ti-contents at $\mu_0 H = 0$ and 3 T, respectively, are plotted for both the 700d- and 900d-bulks in Fig. 2(b) and (c). The J_c at 0 T for the 700d-bulks initially increases with Ti-doping, takes a peak at Ti5%-doping, and decreases with increasing Ti-contents. Ti50%-doping for the 700d-bulk obviously reduces the J_c.

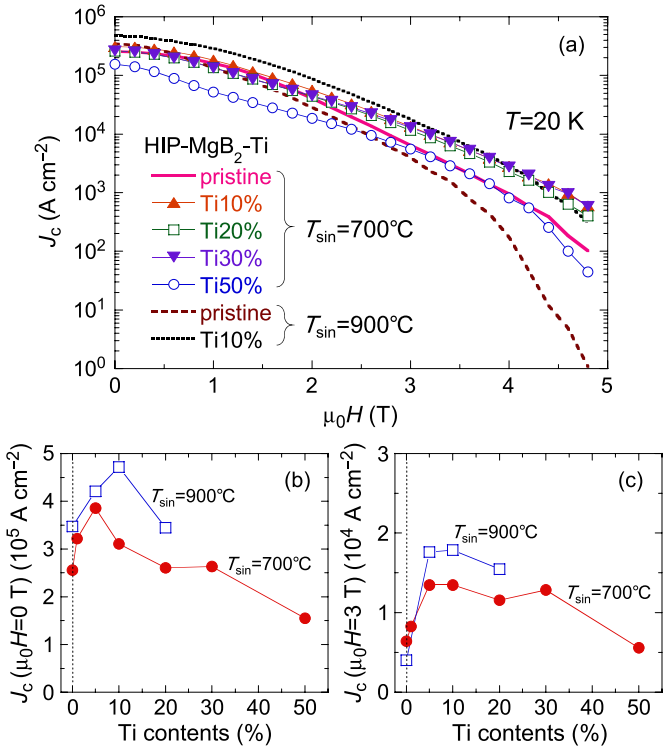

Fig. 2. (a) Magnetic field dependence of the critical current density, $J_c(\mu_0 H)$, at 20 K of the pristine and four Ti-doped MgB_2 bulks sintered at $T_{\rm sin} = 700$ °C. The $J_c(\mu_0 H)$ curves of the MgB_2 bulks with $T_{\rm sin} = 900$ °C for $x = 0$ and 0.1 are also shown, which are referred to in Ref. [8]. Ti contents dependence of J_c at (b) $\mu_0 H = 0$ and (c) 3 T for the Ti-doped MgB_2 bulks with $T_{\rm sin} = 700$ °C and 900 °C.

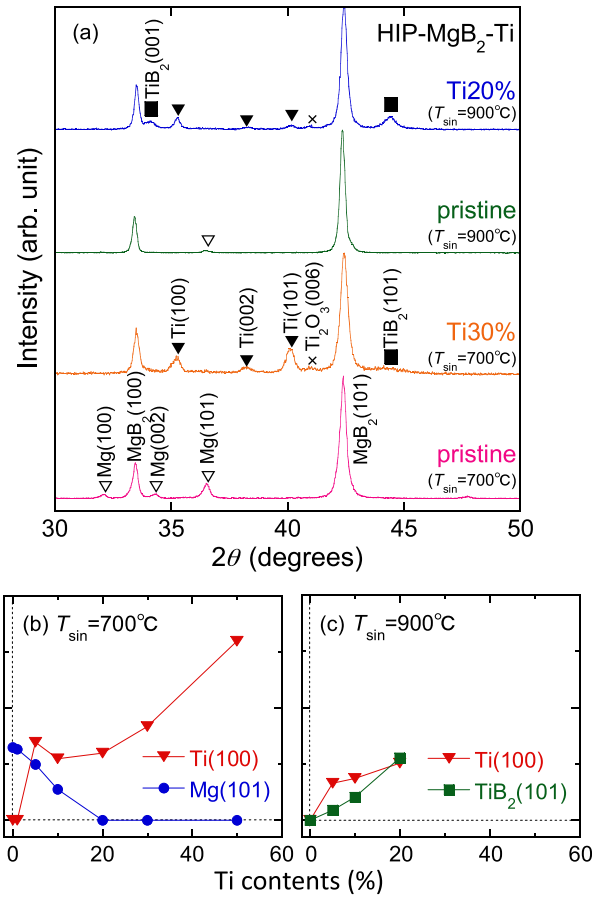

Fig. 3. (a) Powder X-ray diffraction patterns taken at the room temperature for the $Mg_{1-x}Ti_xB_2$ bulks sintered at 700 °C ($x = 0, 0.3$) and 900 °C ($x = 0, 0.2$). Peak intensity ratios of impurity peaks to the main peak of the $MgB_2(101)$ for the bulks with (b) $T_{\rm sin} = 700$ °C and (c) 900 °C.

The similar behavior was also found for the 900d-bulks, in which the Ti10%-doping maximizes J_c. Under 3 T, the J_c is enhanced from 6.4×10^3 A cm^{-2} for the 700d-pristine bulk to $1.2 - 1.4 \times 10^4$ A cm^{-2} for the 700d-Ti5–30% bulks. The somewhat small J_c's of the 700d-Ti10–30% bulks compared to that of 900d-Ti5–20% bulk originates from the reduced volume fraction of MgB_2 for the 700d-bulks. Consequently, the Ti-doping effectively enhanced the $J_c(\mu_0 H)$ in high fields.

Fig. 3(a) shows the powder X-ray diffraction (XRD) patterns for the 700d-bulks ($x = 0, 0.3$) and 900d-bulks ($x = 0, 0.2$) [8]. The MgB_2 phase is dominant for all the bulks. A residual unreacted Mg for both pristine bulks and Ti, Ti_2O_3, TiB_2 for the both Ti-doped bulks appear as the impurity phases. Fig. 3(b) and (c) show the ratios of the peak intensity of the impurities to the $MgB_2(101)$ plane for the 700d- and 900d-bulks, respectively. For the 700d-bulks, the intensity ratio of the Ti(100) abruptly increases from 0 for both the Ti0% and Ti1% to 0.14 for Ti5%, increases moderately with increasing Ti-contents, and finally reached 0.32 for Ti50%. On the other hand, the amount of the Mg phase decreases monotonically with increasing Ti-contents. The tendency of the increase of Ti for the 900d-bulks is resemble to that for the 700d-bulks. The amount of TiB_2 phase increases monotonically with Ti-contents for the 900d-bulks. In contrast to the 900d-Ti-doped bulks, no clear impurity peaks of the TiB_2 phase appeared for the 700d-Ti-doped bulks, indicating that the different types of pinning centers might be created.

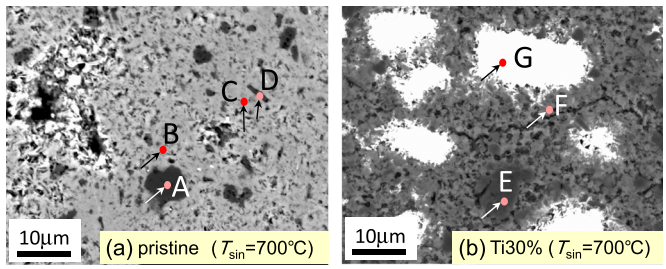

Fig. 4. Backscattered electron (compositional contrast) images of the (a) pristine and (b) Ti30%-doped MgB_2 bulks sintered at 700 °C. The chemical composition was quantitatively examined at the indicated points (A-G).

Fig. 4 shows the backscattered electron (compositional contrast) images for the 700d-bulks ($x = 0, 0.3$). For the 700d-pristine bulk, many dark spots are found in the dominant bright gray area and some darker (black) parts represent the voids. The quantitative chemical composition was analyzed at the indicated points (A-G), which was summarized in Table II. The chemical composition at points A and D are the MgB_y phases with $y = 10.5$ and 6.4, respectively, suggesting that the dark parts are strongly B-enriched compounds, that is, higher borides. The creation of higher borides results in the residual unreacted Mg, as found in the XRD pattern [Fig. 3(a)]. The compositions of

TABLE II
CHEMICAL COMPOSITION OF THE MgB_2 BULKS SINTERED AT 700 °C

	Analyzed position*						
Element	A	B	C	D	E	F	G
Mg	1	1	1	1	1	1	0
B	10.5	2.1	3.3	6.4	9.2	3.1	0
Ti	0	0	0	0	0	0	1

*indicated by point and arrow in Fig. 4

MgB_y with $y = 2.1$ and 3.3, respectively, was obtained for points B and C, therefore the dominant bright gray area is confirmed to be the MgB_2 phase with a small amount of higher borides. For the 700d-Ti30% bulk, the dominant gray area (point F) and the dark region (point E) have the composition of MgB_y with $y = 3.1$ and 9.2, respectively. Therefore, the chemical composition of main and impurity phases for the Ti-doped bulk is almost the same as the nondoped bulk. Quite large bright regions appear in the Ti30% bulk are Ti, because of the composition of Mg : B : Ti = 0 : 0 : 1 at point G. The similar B-enriched MgB_y ($y > 2$) phases and large Ti precipitates were also observed for the Ti-doped 900d-bulks [8]. The B-rich area in the MgB_2 matrix is probably nanometric size smaller than the present resolution of FE-EPMA. Therefore, the present nanometric B-rich particles are expected to trap effectively the vortices. Several reports suggested that an oxide in the starting Mg powder due to the high affinity of Mg to O often forms the Mg-B-O inclusions with nanometer-size as the pinning centers [17], [18]. Furthermore, Prikhna *et al.* pointed out that the Ti-doping reduced the oxygen content in the MgB_2 matrix by absorbing oxygen and concurrently promoted the creation of the nanometric Mg-B-O inclusions, which resulted in the further J_c-increase. [18]. In addition, an accumulated B layer on the Ti particles, which was found in 900d-Ti-doped bulks [8], is not confirmed for the 700d-Ti30% bulks, which suggests no TiB_2 phases in the bulk. To clarify precisely the pinning mechanism of the Ti-doped bulk without TiB_2, the role of oxygen should be examined.

Fig. 5 shows the electron backscattered diffraction (EBSD) images for the pristine and Ti10% bulks for $T_{\rm sin} = 700$ °C and 900 °C. The mosaic structure with various colors suggests that the bulk consists of the randomly oriented grains. The grain size of MgB_2 for the 700d-bulks is smaller than that for the 900d-bulks, which comes from the suppression of the grain growth due to the lower sintering temperature. The Ti-doping evidently further reduced the grain size of MgB_2 for both 700d- and 900d-bulks. An unanalyzed area shown by black color indicates amorphous and/or the quite fine grain smaller than the resolution limit of 50 nm for the EBSD apparatus. This results in difficulties in indexing EBSD patterns in these regions. This area increases in the overall region for the 700d-bulks, especially for the Ti10% bulk. The wide unanalyzed areas were found around the Ti particles for the 900d-Ti10% bulk indicated by the thick arrows, in which the TiB_2 phase was included [8]. Both smaller MgB_2 grains and the increase of the amorphous phase bring about the fact that the 700d-Ti-doped bulks with the relatively low $f \sim 80\%$ show the high B_T values comparable to those of the highly dense 900d-Ti-doped bulks ($f \geq 90\%$). Therefore, the 700d-Ti-doped bulks with $f \geq 90\%$ should offer at least 10% higher B_T with respect to the present bulks. The origin of the grain refining by Ti-doping in the 700d-bulk without the TiB_2 phase is believed to differ from the TiB_2 mechanism [16].

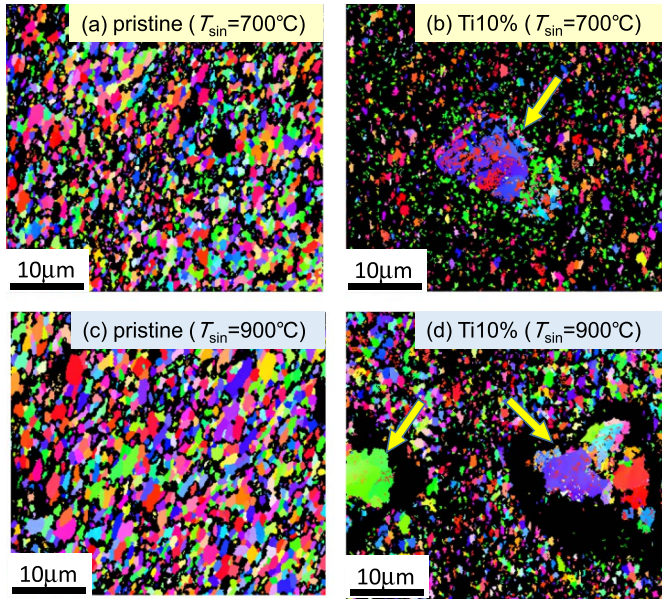

Fig. 5. Electron backscattered diffraction images for the (a) pristine and (b) Ti10%-doped MgB_2 bulks sintered at $T_{\rm sin} = 700$ °C and for the (c) pristine and (d) Ti10%-doped MgB_2 bulks at $T_{\rm sin} = 900$ °C. The thick arrows in (b) and (d) indicate Ti particles.

IV. SUMMARY

We have studied the trapped field properties and the microstructure for the Ti-doped MgB_2 bulks sintered at $T_{\rm sin} = 700$ °C by the *in situ* HIP method compared to those sintered at $T_{\rm sin} = 900$ °C. The trapped fields, B_T's, for the $T_{\rm sin} = 700$ °C bulks with relatively low filling factor of $f = 70$–90% were comparable with those for the $T_{\rm sin} = 900$ °C bulks with higher $f \geq 90\%$. The critical current densities, $J_c(\mu_0 H)$'s, were also almost independent of both the sintering temperature and Ti-contents (except for Ti50%-doping), which is consistent with the results of B_T properties. The quantitative analysis of the chemical composition suggested that the nonsuperconducting nanometric particles of higher borides, MgB_y ($y > 2$), existed in the $T_{\rm sin} = 700$ °C bulk. The smaller MgB_2 grains and/or larger amount of the amorphous MgB_2 phase were obtained for the $T_{\rm sin} = 700$ °C bulks compared to the $T_{\rm sin} = 900$ °C bulks by both the lower sintering temperature and Ti-doping. The increase of these pinning centers resulted in the sintering temperature independent B_T. To clarify the mechanism of the grain refining by Ti-doping for the $T_{\rm sin} = 700$ °C bulks without TiB_2 phase, further study is now in progress.

ACKNOWLEDGMENT

We would like to acknowledge Dr. H. Teshima of Nippon Steel & Sumitomo Metal Corporation for his assistance in the preparation of the MgB_2 bulks using the HIP furnace and Mr. K. Nonaka of Iwate University for his help in the microstructure analysis using FE-EPMA.

REFERENCES

[1] M. Murakami, M. Morita, K. Doi, and K. Miyamoto, "A new process with the promise of high J_c in oxide superconductors," *Jpn. J. Appl. Phys.*, vol. 28, no. 7, pp. 1189–1194, Jul. 1989.

[2] R. V. Viznichenko *et al.*, "Temperature dependence of the trapped magnetic field in MgB_2 bulk superconductors," *Appl. Phys. Lett.*, vol. 83, no. 21, pp. 4360–4362, Nov. 2003.

[3] E. Perini *et al.*, "Magnetic field trapping in MgB_2 bulks and inserts," *IEEE Trans. Appl. Supercond.*, vol. 21, no. 3, pp. 2690–2693, Jun. 2011.

[4] T. Naito, T. Sasaki, and H. Fujishiro, "Trapped magnetic field and vortex pinning properties of MgB_2 superconducting bulk fabricated by a capsule method," *Supercond. Sci. Technol.*, vol. 25, no. 9, Jul. 2012, Art. no. 095012.

[5] J. H. Durrell *et al.*, "A trapped field of > 3 T in bulk MgB_2 fabricated by uniaxial hot pressing," *Supercond. Sci. Technol.*, vol. 25, no. 11, Oct. 2012, Art. no. 112002.

[6] T. Sasaki, T. Naito, and H. Fujishiro, "Trapped magnetic field of dense MgB_2 bulks fabricated under high pressure," *Phys. Procedia*, vol. 45, pp. 93–96, 2013.

[7] A. Yamamoto, A. Ishihara, M. Tomita, and K. Kishio, "Permanent magnet with MgB_2 bulk superconductor," *Appl. Phys. Lett.*, vol. 105, no. 3, Jul. 2014, Art. no. 032601.

[8] T. Naito, T. Yoshida, and H. Fujishiro, "Ti-doping effects on magnetic properties of dense MgB_2 bulk superconductors," *Supercond. Sci. Technol.*, vol. 28, no. 9, Jul. 2015, Art. no. 095009.

[9] M. Kambara *et al.*, "High intergranular critical currents in metallic MgB_2 superconductor," *Supercond. Sci. Technol.*, vol. 14, no. 4, pp. L5–L7, Apr. 2001.

[10] D. C. Larbalestier *et al.*, "Strongly linked current flow in polycrystalline forms of the superconductor MgB_2," *Nature*, vol. 410, no. 6825, pp. 186–189, Mar. 2001.

[11] A. Murakami *et al.*, "Low-temperature mechanical properties of bulk MgB_2 fabricated by hot isostatic pressing," *Phys. Procedia*, vol. 67, pp. 982–986, 2015.

[12] J. Nagamatsu, N. Nakagawa, T. Muranaka, Y. Zenitani, and J. Akimitsu, "Superconductivity at 39 K in magnesium diboride," *Nature*, vol. 410, no. 6824, pp. 63–64, Mar. 2001.

[13] S. S. Indrakanti *et al.*, "Hot isostatic pressing of bulk magnesium diboride: Mechanical and superconducting properties," *Philos. Mag. Lett.*, vol. 81, no. 12, pp. 849–857, Dec. 2001.

[14] G. Fuchs *et al.*, "High trapped fields in bulk MgB_2 prepared by hot-pressing of ball-milled precursor powder," *Supercond. Sci. Technol.*, vol. 26, no. 12, Nov. 2013, Art. no. 122002.

[15] Y. Zhao *et al.*, "High critical current density of MgB_2 bulk superconductor doped with Ti and sintered at ambient pressure," *Appl. Phys. Lett.*, vol. 79, no. 8, pp. 1154–1156, Aug. 2001.

[16] Y. Zhao *et al.*, "Nanoparticle structure of MgB_2 with ultrathin TiB_2 grain boundaries," *Appl. Phys. Lett.*, vol. 80, no. 9, pp. 1640–1642, Mar. 2002.

[17] Y. Zhu *et al.*, "Microstructure and structural defects in MgB_2 superconductor," *Phys. C, Supercond.*, vol. 356, no. 4, pp. 239–253, Aug. 2001.

[18] T. Prikhna *et al.*, "Influence of nanostructural inhomogeneities on superconducting characteristics of MgB_2," *J. Supercond. Novel Magn.*, vol. 28, no. 2, pp. 525–530, Feb. 2015.

[19] C. P. Bean, "Magnetization of hard superconductors," *Phys. Rev. Lett.*, vol. 8, no. 6, pp. 250–253, Mar. 1962.

[20] E. M. Gyorgy, R. B. van Dover, K. A. Jackson, L. F. Schneemeyer, and J. V. Waszczak, "Anisotropic critical currents in $Ba_2YCu_3O_7$ analyzed using an extended Bean model," *Appl. Phys. Lett.*, vol. 55, no. 3, pp. 283–285, Jul. 1989.

[21] T. Prikhna *et al.*, "High-pressure synthesis of MgB_2 with addition of Ti," *Phys. C, Supercond.*, vol. 402, no. 3, pp. 223–233, Feb. 2004.